ACTA IMEKO
ISSN: 2221-870X
December 2023, Volume 12, Number 4, 1 - 6

Performance evaluation of pocket echo using an ultrasonic accuracy control phantom

Norimitsu Shinohara[1], Yohan Kondo[2]

[1] *Department of Radiological Technology, Faculty of Health Sciences, Gifu University of Medical Science, 1-795 Ichihiraga, Nagamine, Seki City, Gifu Seki City, Gifu City, Gifu Prefecture, 501-3892, Japan*
[2] *Graduate School of Health Sciences, Niigata University, 2-746, Asahimachidori, Chuouku, Niigata 951-8518, Japan*

ABSTRACT
In addition to being used in hospitals, ultrasound systems are used in many other medical settings such as disaster relief and home care. In these types of settings, it is important to be able to perform a large number of examinations easily and efficiently. Portable ultrasound systems can be used to meet such needs. The evaluation of ultrasound systems has been driven by the development of accuracy control methods used in breast examinations. This study aimed to evaluate the performance of portable ultrasound systems that have not yet been fully investigated. The performance of two ultrasound systems was evaluated using three measures. For physical evaluation, the change in the mean pixel value of the target and the contrast-to-noise ratio were obtained for each ultrasound system. Statistical analyses were performed to compare these measures between the two systems. For visual evaluation, a receiver operating characteristic analysis was performed. The results of the physical and visual evaluations showed no statistically significant differences between the portable ultrasound systems we evaluated and those that are commonly used in clinical practice.

Section: RESEARCH PAPER

Keywords: portable ultrasound system; ultrasound system performance; disaster medicine; home care

Citation: Norimitsu Shinohara, Yohan Kondo, Performance evaluation of pocket echo using an ultrasonic accuracy control phantom, Acta IMEKO, vol. 12, no. 4, article 43, December 2023, identifier: IMEKO-ACTA-12 (2023)-04-43

Section Editor: Laura Fabbiano, Politecnico di Bari, Italy

Received October 11, 2022; **In final form** December 12, 2023; **Published** December 2023

Funding: This work was supported by the Japan Society for the Promotion of Science (JSPS) KAKENHI, Grant Number 20K11068.

Corresponding author: Norimitsu Shinohara, e-mail: shinohara@u-gifu-ms.ac.jp

1. INTRODUCTION

Diagnostic ultrasound systems can be used to noninvasively visualize the interior of the body in real-time. These systems are used in not only hospitals but also various medical settings, including in the provision of medical assistance during disasters and home care [1]-[3]. As no special qualifications are required to use diagnostic ultrasound systems and radiation exposure is not a problem, ultrasonography may be used for simple examinations of disaster victims while they reside in evacuation centers. In situations where medical support outside a medical facility is required, a large number of examinations may need to be performed easily and efficiently [4]-[6]. For this, portable ultrasound systems that are small and easy to carry are advantageous [7], [8].

In a previous study evaluating portable ultrasound systems, Dalen et al. reported high sensitivity and specificity in the evaluation of pleural effusions using a hand-held device [9]. Del Medico et al. reported that high sensitivity and specificity can be obtained if cholelithiasis is diagnosed by experts using portable ultrasound systems [10]. Kameda et al. found excellent agreement between portable ultrasound systems and clinically used ultrasound equipment in diagnosing the presence of hydronephrosis [11]. Esposito et al. reported that portable ultrasound systems are a reliable screening tool for early detection of abdominal aortic aneurysms by measuring the diameter of the abdominal aorta [12]. These papers show that there is overall agreement in diagnosis between portable ultrasound systems and clinically used ultrasound equipment and that portable ultrasound systems may be a valuable supplement to the examination, but the evidence is also insufficient evidence exists to make standardized comparisons [13], [14]. These are only subjective clinical evaluations limited to individual clinical problems, not objective evaluations based on image quality measurements.

Previous studies that evaluated the image quality performance of ultrasound systems have focused on the development of accuracy control methods for breast ultrasound screening [15]-[18]. However, studies that evaluated the performance of portable ultrasound systems could not be confirmed within the scope of our research. Therefore, verification is necessary.

The purpose of this study was to objectively evaluate the image quality performance of a pocket-sized portable ultrasound system using an ultrasound accuracy control phantom.

2. MATERIALS AND METHODS

2.1. Materials

Two ultrasound systems were evaluated in the present study. The first was a portable ultrasound system, the Miruco pocket echo (pocket echo), manufactured by Sigmax, Tokyo, Japan (Figure 1). The second was the SONIMAGE HS1 (standalone ultrasound), manufactured by Konica Minolta, Inc., Tokyo, Japan, which is commonly used in clinical practice (Figure 2).

2.2. Imaging target

In the present study, the breast ultrasound accuracy control phantom US-4 (the phantom), manufactured by Kyoto Scientific, Kyoto, Japan, was used as the imaging target (Figure 3). Table 1 shows the specifications for this phantom at an internal temperature of 25°C. The phantom had four different target areas embedded 1 and 2 cm below the surface. Grayscale targets, embedded in a mass target block, were used. Figure 4 shows examples of the grayscale targets taken by the two ultrasound systems. The 10 grayscale targets were numbered 1–10, from the low-echo target to the high-echo target. These 10 targets have different acoustic impedance ratios to the base material, which, in ascending order starting from target 1, are 1/30, 1/20, 1/10, 1/5, 1/3, 1/2, 1, 5, 10, and 30. Target 7 has an acoustic impedance ratio of 1 to the base material. Therefore, the contrast between the target and base material did not appear in the image, and the presence of the target could not be confirmed.

Figure 1. Pocket echo.

Figure 2. Standalone ultrasound.

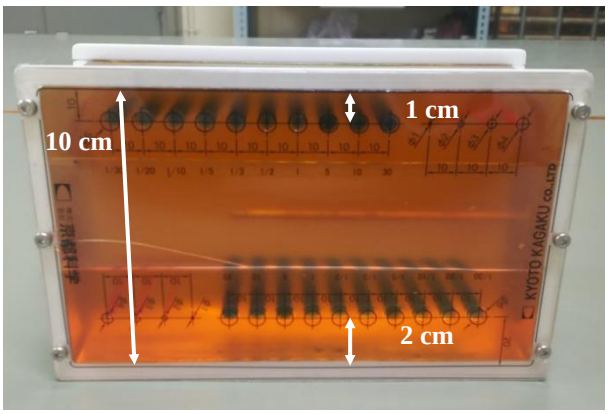

Figure 3. Breast ultrasound accuracy control phantom (mass target block).

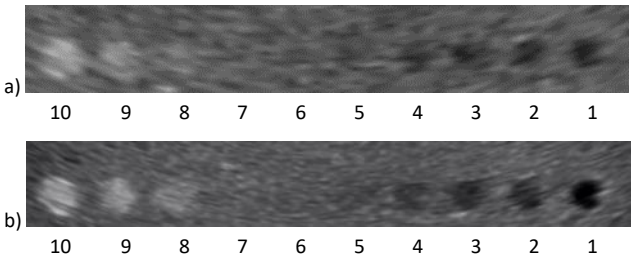

Figure 4. Grayscale target images (numbers indicate target numbers): a) pocket echo and b) standalone ultrasound.

2.3. Imaging conditions

Owing to the unique technologies used by each manufacturer, it is difficult to perfectly match the imaging conditions of the different ultrasound systems. Therefore, we selected one mode for each observation site and compared the results based on the conditions in that mode using a convex probe. For the pocket echo, the deep mode was selected, whereas for the standalone ultrasound, the abdominal mode was selected. The frequency was set to 3.5 MHz as the pocket echo did not allow the switching of frequencies. For scanning, a coupling gel was used and no holder was used to maintain the probe stationary on the phantom surface. The gain was adjusted such that the luminance differences between the 10 targets could be observed sequentially. The gain was set to 77 for the pocket echo and 22 for the standalone ultrasound. The targets to be evaluated were targeted at a distance of 8 cm for deep evaluation and were imaged using a convex probe so that all 10 targets could be captured in a single image (Figure 5).

For each ultrasound system, the grayscale targets were imaged under the same conditions 20 times. Figure 6 shows the images taken using the pocket echo and standalone ultrasound. The resolutions of the images taken by the two systems were 0.4 mm/pixel for the pocket echo and 0.3 mm/pixel for the standalone ultrasound.

Table 1. Phantom specifications at an internal temperature of 25°C.

Sound velocity	1,437 m/s
Attenuation coefficient	0.57 dB/cm MHz
Acoustic impedance	1.38 Pa·s/m^3
Target diameter	6 mm

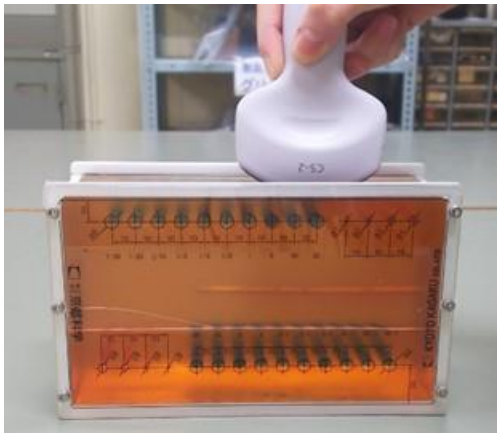

Figure 5. Taking an image.

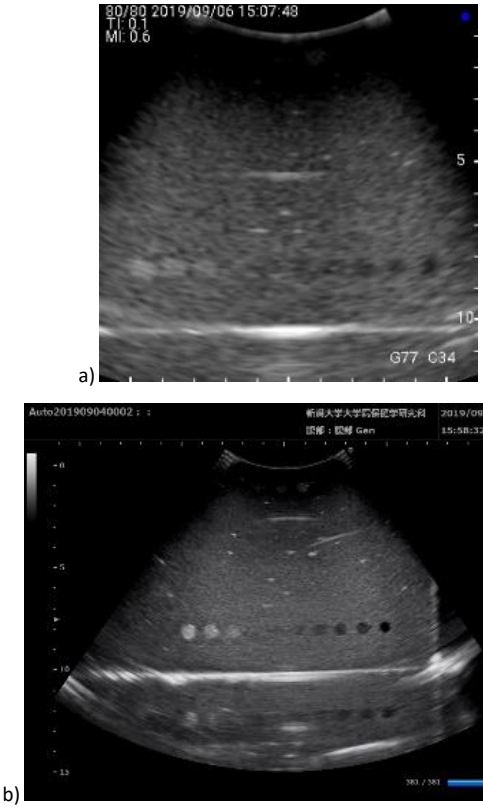

Figure 6. Ultrasound images: a) pocket echo, and b) standalone ultrasound.

2.4. Evaluated items

Figure 7 shows a flowchart of the physical evaluation process. For physical evaluation, the change in the average pixel value of the target and the contrast-to-noise ratio (CNR) were obtained. Subsequently, statistical analysis was performed on the measured values of the two devices. For visual evaluation, a receiver operating characteristic (ROC) analysis was performed. The details of the physical and visual evaluations are described below.

2.5. Physical evaluation (Change in average pixel value for each target)

To evaluate the physical characteristics of the ultrasound systems, we examined whether each luminance change between the 10 targets was captured in the same way by both devices. A total of 40 images (20 images per device) were used for this measurement. For each image obtained, the region of interest

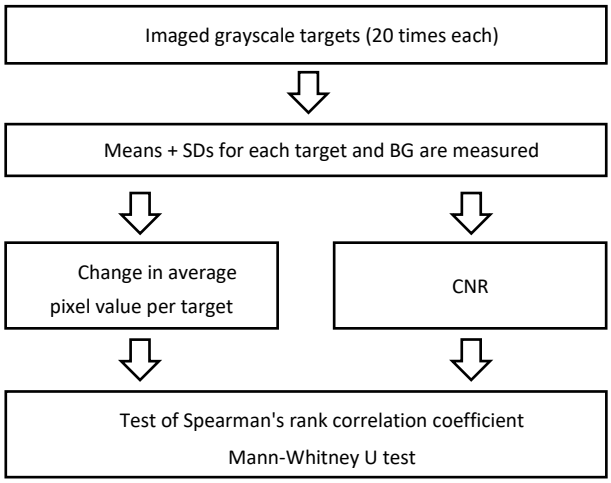

Figure 7. Flowchart of the physical evaluation.

Figure 8. ROI setup: solid line, ROI in the target (3-mm diameter); dotted line, same size ROI in the background.

(ROI) was set as the target and its background (a point directly above each target) (Figure 8). The mean (E_i) and standard deviation (σ_i) of the pixel values in each ROI were calculated. The size of the ROI was the same for each device, that is, a circle with a diameter of 3 mm (7.5 pixels for the pocket echo and 10 pixels for the standalone ultrasound). The average value of the ROI measured from each of the 20 images per device was used as the average ROI value for each target. E_i is the average pixel value of each target.

2.6. Physical evaluation (CNR)

The following equation (1) was used to calculate CNR [7]:

$$CNR = \frac{|\langle E_T\rangle - \langle E_B\rangle|}{\sqrt{\sigma^2_{\langle E_T\rangle} + \sigma^2_{\langle E_B\rangle}}}, \tag{1}$$

where $\langle E_T\rangle$ and $\sigma_{\langle E_T\rangle}$ are the weighted mean and standard deviation, respectively, obtained by weighting E_i and σ_i for each target. $\langle E_B\rangle$ is the weighted mean of the background region and $\sigma_{\langle E_B\rangle}$ is the corresponding weighted standard deviation. The weighted mean $\langle E_T\rangle$was calculated using equation (2), and the weighted standard deviation $\sigma_{\langle E_T\rangle}$ was calculated using equation (3)

$$\langle E_T\rangle = \frac{\sum_i w_i E_i}{\sum_i w_i}, \tag{2}$$

$$\sigma_{\langle E_T\rangle} = \frac{1}{\sqrt{\sum_i w_i}}. \tag{3}$$

Here, w_i was defined as follows:

$$w_i = \frac{1}{\sigma_i^2}. \tag{4}$$

2.7. Statistical analysis

Spearman's rank correlation coefficient and Mann-Whitney U tests were performed to evaluate changes in the mean pixel values of the targets and CNR measurements between the pocket echo and standalone ultrasound. The Mann-Whitney U test is a nonparametric method used to test for differences in the distribution of two non-corresponding groups of data. The null hypothesis for the present study was that there is no difference between the measurements of the two instruments, while the alternative hypothesis was there is a difference between the measurements of the two instruments. For both the tests, the risk rate was set at 5 %. The statistical software program EZR (Easy R) [19] was used to perform all statistical analyses.

2.8. Visual assessment (Observers and observed samples)

Ten students training to be technologists (eight fourth-year students from the Department of Radiological Technology, Faculty of Health Sciences, Niigata University School of Medicine and one first- and one second-year student from the Department of Radiological Technology, Graduate School of Health Sciences, Niigata University) acted as observers for the visual assessment component. This was a simple observation to judge whether there was a signal in the center of the image. Hence, non-specialist students would have no problem making the observations. A total of 40 images (20 images per system) were obtained using the pocket echo and standalone ultrasound to prepare the observation samples. The target utilized for these observations was the most difficult to see out of the 10 targets (target 6). Briefly, 1 cm × 1 cm squares were cut from each image, and the area of target 6, as well as the area directly above target 6, were used as the samples. There were 80 observation samples, consisting of 20 images with and 20 without signals for each ultrasound system. Figure 9 shows the preparation of the observation samples.

2.9. Visual assessment (Observer experiment)

Of the prepared samples, eight images were used for training: two images with and two without signals for each device. In total, 72 images were used for the observation evaluation: 18 images with and 18 without signals created from images taken by the standalone ultrasound and 18 images with and 18 without signals created from images taken by the pocket echo.

The observers were shown the samples (Figure 10) one by one at random on the display and asked to observe each sample within 10 s. The continuous confidence method, which assigns a score to an observed sample without categorizing it, was used for the evaluation. A 5-cm scale bar was set up, and the participants were asked to mark the right side of the bar as their confidence in the presence of a signal increase and the left side of the bar as their confidence in the absence of a signal increased. The positions of the marks were measured, and the score for each image was calculated. For example, a mark at 3 cm was assigned 30 points. (= 30 mm).

2.10. Visual assessment (ROC analysis)

ROCKIT and LABMRMC were used for the ROC analysis, which are ROC analysis software programs developed by Metz et al. [20] at the University of Chicago. The scores obtained from the observer experiment were input into ROCKIT to obtain the true and false positive rates for each observer. An average ROC curve was generated using the average method. The jackknife method [21] was used to test for statistical significance using LABMRMC, with a risk rate of 5 %.

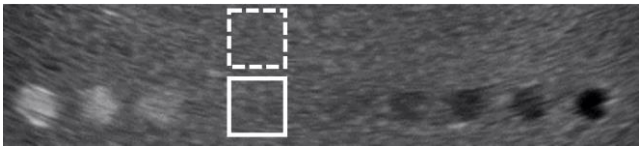

Figure 9. Sample preparation: squares indicate regions of interest (1 cm × 1 cm); solid line, with signal, and dashed line, without signal.

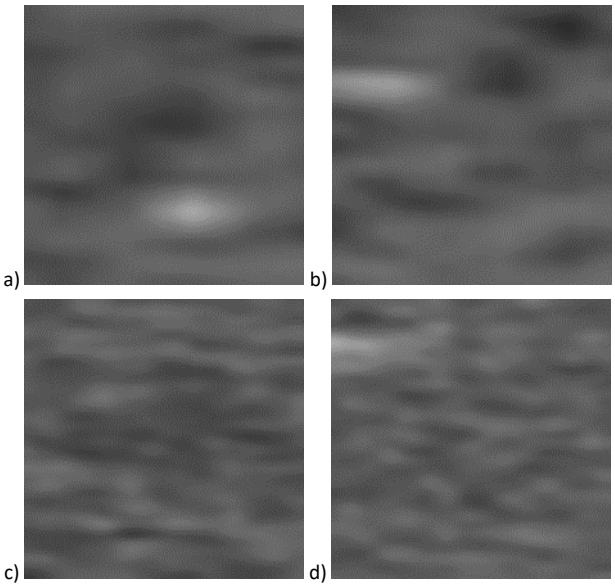

Figure 10. Examples of observed samples: a) pocket echo with signal, b) pocket echo without signal, c) standalone ultrasound with signal, and d) standalone ultrasound without signal.

3. RESULTS

3.1. Changes in the average pixel value of the target

Table 2 shows the measured mean pixel values and standard deviations of the targets obtained using each device. Figure 11 shows the change in the average pixel value of the target obtained using each device. When applied to the data obtained from the two ultrasound systems, Spearman's rank correlation coefficient test yielded a correlation coefficient of 0.988 ($p < 0.01$), while the Mann-Whitney U test yielded $p = 0.912$.

3.2. CNR

Table 3 shows the calculated CNR of the targets obtained using each device. Spearman's rank correlation coefficient test of the CNRs from each target, obtained for both ultrasound devices, is shown in Figure 12. The Mann-Whitney U test yielded a p-value of 0.853.

Table 2. Measured average pixel value and standard deviation of the targets.

No. of Target	Standalone		Pochet echo	
	Average	SDs	Averages	SDs
1	4.26	1.99	40.50	3.33
2	41.61	7.03	54.78	4.59
3	49.19	4.20	54.05	3.77
4	62.80	8.68	65.81	5.27
5	72.12	5.24	72.83	5.87
6	80.80	3.73	77.53	3.65
7	89.59	3.68	92.40	5.18
8	121.99	6.46	111.87	6.69
9	138.31	7.53	132.38	5.23
10	154.39	7.60	150.20	4.90

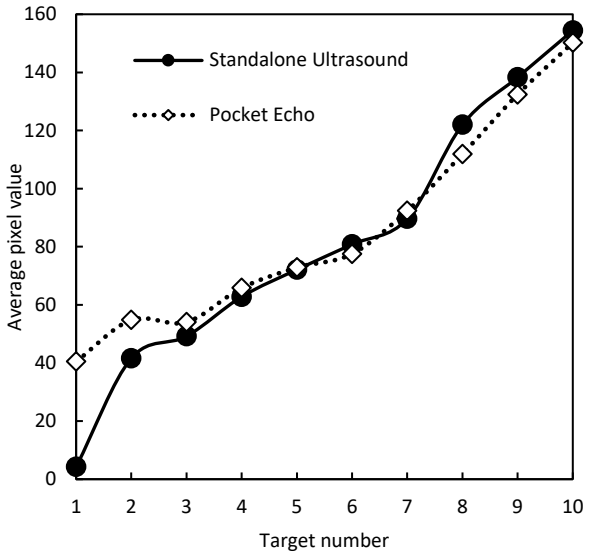

Figure 11. Variations of the average pixel value of targets.

Table 3. CNR of the calculated target.

No. of Target	Standalone	Pochet echo
1	36.41	21.21
2	20.51	15.73
3	16.02	10.99
4	10.18	6.55
5	6.42	4.42
6	4.44	5.27
7	0.07	2.67
8	9.78	9.87
9	15.11	17.76
10	20.95	25.09

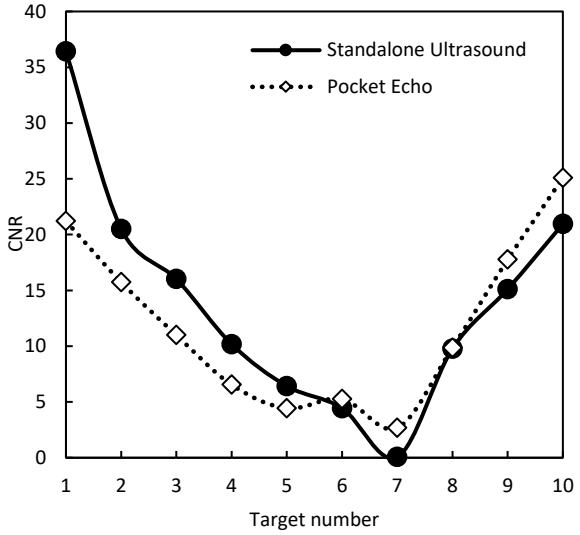

Figure 12. CNR of targets.

3.3. ROC analysis

The average ROC curves of the 10 observers for each device are shown in Figure 13. The ROC curve indicates that the signal detectability is higher as it approaches the upper left corner and lower as it approaches the positive diagonal. Therefore, a larger area under the ROC curve (AUC) indicates a higher detectability, which was $AUC = 0.834$ for the standalone ultrasound and $AUC = 0.759$ for the pocket echo. The jackknife method yielded a p-value of 0.225.

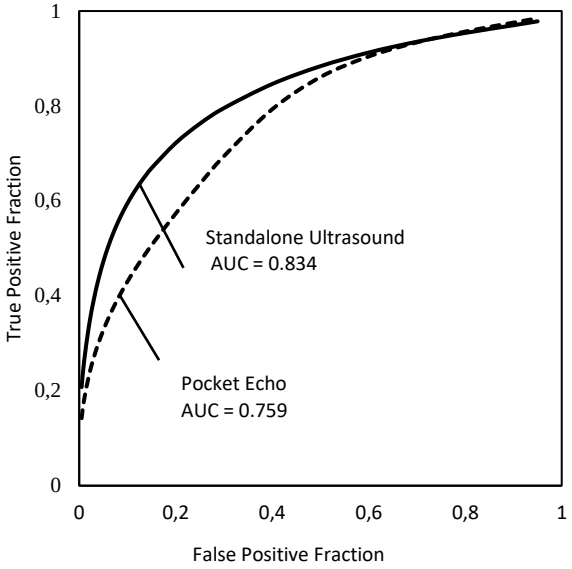

Figure 13. Receiver operating characteristic curve.

4. DISCUSSION

The Spearman's rank correlation coefficient test, which was used to evaluate the changes in the mean pixel values of the targets obtained from each device, resulted in a correlation coefficient of 0.988 ($p < 0.01$). This suggests that there was a significant correlation between the measured values of the two devices. The Mann-Whitney U test resulted in $p > 0.05$. Thus, the null hypothesis, there is no difference between the measurements of the two instruments, was not rejected. Considering these results, there was no significant difference between the measurements obtained from the two ultrasound systems; thus, there was no difference between the two instruments with respect to the change in the average pixel values of the targets.

Similarly, the evaluation of the CNR for each device using Spearman's rank correlation coefficient test yielded a correlation coefficient of 0.927 ($p < 0.01$). This suggests that there was a significant correlation between the measured values of the two instruments. In contrast, the Mann-Whitney U test resulted in $p > 0.05$. Therefore, the null hypothesis, there is no difference between the measurements of the two instruments, was not rejected. Considering these results, there was no significant difference in the measured values of the two instruments; thus, there was no difference in the CNR between the two ultrasound systems.

We also found that the statistical significance test for the ROC curves of the two devices yielded a result of $p > 0.05$, and no significant difference was observed between the pocket echo and standalone ultrasound. Hence, there was no difference in the visualization of the targets between the two devices.

As a limitation of this experiment, it is not possible to analyze the uncertainty of the measured values in this experiment. This is due to the fact that the target value of the measurement is not absolute and that the two ultrasonic devices do not output the same value due to multiple factors such as concentration

resolution and pretreatment. Therefore, this experiment only investigates the similarity in the trend of the output values of each device as the acoustic impedance changes. In addition, this experiment was conducted using a unique model, and verification using a large number of models is necessary.

5. CONCLUSIONS

This study evaluated the performance of the pocket echo and standalone ultrasound using an ultrasonic accuracy control phantom. The objective assessment using the average pixel value of the target and CNR showed no statistically significant difference in the quality of the images produced by the two instruments. Visual assessment using ROC analysis also showed no statistically significant differences. Given that the results of the present study showed that the performance of the pocket echo was not inferior to that of the standalone ultrasound, the inexpensive and easily portable pocket echo is expected to be actively utilized for use for medical support during disasters and in-home medical care.

ACKNOWLEDGEMENT

Here persons of the authors would like to thank Hikaru Kawai for assisting with the study.

REFERENCES

[1] M. Shogenji, M. Dai, J. Sugama, Y. Fukumura, K. Shima, Comparison of bladder volume evaluation by pocket-sized ultrasound devices. J Nurs Sci and Eng. 2016;3(2), pp. 118–22. [In Japanese]
DOI: 10.24462/jnse.3.2_118

[2] P. J. Mariani, J. A. Setla, Palliative ultrasound for home care hospice patients, Academic Emergency Medicine, 2010; 17(3), pp. 293-296.
DOI: 10.1111/j.1553-2712.2009.00678.x

[3] S. Vilanova-Rotllan, B. Kostov, M. J. Giner Martos, J. Benavent-Àreu, A. Sisó-Almirall, Feasibility study of abdominal ultrasound using hand-held devices in homecare services, Medicina Clínica (English Edition), 2022; 158(8), pp. 361-365.
DOI: 10.1016/j.medcli.2021.03.038

[4] S. M. Wydo, M. J. Seamon, S. W. Melanson, P. Thomas, D. P. Bahner, S. P. Stawicki, Portable ultrasound in disaster triage: a focused review, European Journal of Trauma and Emergency Surgery, 2016; 42, pp. 151-159.
DOI: 10.1007/s00068-015-0498-8

[5] Hwang Juin-Jet, J. Quistgaard, J. Souquet, L. A. Crum, Portable ultrasound device for battlefield trauma, IEEE Ultrasonics Symposium, Sendai, Japan, 5-8 October 1998. Proc. (Cat. No. 98CH36102), 1998, pp. 1663-1667.
DOI: 10.1109/ULTSYM.1998.765266

[6] T. Itabashi, H. Chiba, K. Abe, S. Tanaka, S. Masunaga, M. Nagasawa, S. Ueda, Diagnosis algorithm of deep vein thrombosis (DVT) medical examination needed at a large-scale disaster. Japanese J Med Technol. 2017;66(5), pp. 449–62.
DOI: 10.14932/jamt.17-94

[7] A. Neesse, A. Jerrentrup, S. Hoffmann, A. Sattler, C. Görg, C. Kill, T. M. Gress, S. Kunsch, Prehospital chest emergency sonography trial in Germany: a prospective study, European Journal of Emergency Medicine, 2012; 19(3), pp. 161-166.
DOI: 10.1097/mej.0b013e328349edcc

[8] F. J. Neves Mancuso, V. N. Siqueira, V. A. Moisés, A. F. Teixeira Gois, A. A. V. de Paola, A. C. Camargo Carvalho, O. Campos, Focused cardiac ultrasound using a pocket-size device in the emergency room, Arquivos brasileiros de cardiologia, 2014, 103, pp. 530-537.
DOI: 10.5935/abc.20140158

[9] H. Dalen, G. H. Gundersen, K. Skjetne, H. H. Haug, J. O. Kleinau, T. M. Norekval, T. Graven, Feasibility and reliability of pocket-size ultrasound examinations of the pleural cavities and vena cava inferior performed by nurses in an outpatient heart failure clinic, European Journal of Cardiovascular Nursing, 2015; 14(4), pp. 286-293.
DOI: 10.1177/1474515114547651

[10] M. Del Medico, A. Altieri, G. Carnevale-Maffè, P. Formagnana, F. Casella, M. Barchiesi, M. Bergonzi, C. Vattiato, G. Casazza, C. Cogliati, Pocket-size ultrasound device in cholelithiasis: diagnostic accuracy and efficacy of short-term training, Internal and Emergency Medicine, 2018; 13, pp.1121-1126.
DOI: 10.1007/s11739-018-1901-3

[11] T. Kameda, K. Uebayashi, K. Wagai, F. Kawai, N. Taniguchi, Assessment of the renal collecting system using a pocket-sized ultrasound device, Journal of Medical Ultrasonics, 2018, 45, pp. 577-581.
DOI: 10.1007/s10396-018-0881-2

[12] R. Esposito, F. Ilardi, V. Schiano Lomoriello, R. Sorrentino, V. Sellitto, G. Giugliano, G. Esposito, B. Trimarco, M. Galderisi, Identification of the main determinants of abdominal aorta size: a screening by Pocket Size Imaging Device, Cardiovascular Ultrasound, 2017; 15(1), pp. 1-7.
DOI: 10.1186/s12947-016-0094-z

[13] A. Rykkje, J. F. Carlsen, M. B. Nielsen, Hand-Held Ultrasound Devices Compared with High-End Ultrasound Systems: A Systematic Review, Diagnostics. 2019; 9(2):61.
DOI: 10.3390/diagnostics9020061

[14] K. F. Stock, B. Klein, D. Steubl, C. Lersch, U. Heemann, S. Wagenpfeil, F. Eyer, D.-A.e Clevert, Comparison of a pocket-size ultrasound device with a premium ultrasound machine: diagnostic value and time required in bedside ultrasound examination, Abdominal imaging, 2015; 40, pp. 2861-2866.
DOI: 10.1007/s00261-015-0406-z

[15] M. Sakurai, M. Fukuda, E. Imamura, et al., Accuracy control and quality control of diagnostic ultrasound systems using phantoms for accuracy control and creation of educational phantoms, J Japanese Soc Breast Cancer Screen. 2008;17(1), pp. 52–59.

[16] N. Shinohara, N. Kamiya, A. Wada, T. Morita, Development of an accuracy control tool for mass target analysis of a dedicated phantom for breast ultrasound system, J Japanese Soc Breast Cancer Screen. 2013;22(2), pp. 336–342. [In Japanese]
DOI: 10.3804/jjabcs.22.336

[17] Y. Yamane, N. Kamiya, N. Shinohara, Development of an automatic analysis tool for accuracy control phantoms for mammary ultrasound systems, 10th Inf Sci Technol Forum, 2011, pp. 531–532.

[18] E. Sassaroli, C. Crake, A. Scorza, D.-S. Kim, M.-A. Park, Image quality evaluation of ultrasound imaging systems: advanced B-modes. J Appl Clin Med Phys. 2019, 20(3), pp. 115–24.
DOI: 10.1002/acm2.12544

[19] Kanda Y. Investigation of the freely available easy-to-use software 'EZR' for medical statistics. Bone Marrow Transplant. 2013, 48(3), pp. 452–8.
DOI: 10.1038/bmt.2012.244

[20] Metz's ROC Software. Online [Accessed September 2023] http://imgcom.jsrt.or.jp/rocGroup/

[21] D. D. Dorfman, K. S. Berbaum, C. E. Metz, Receiver operating characteristic rating analysis: generalization to the population of readers and patients with the jackknife method, Investigative radiology, 1992, 27(9), pp. 723-731, PMID: 1399456.